2019

Coupled cfd-dem modelling of mine dust dispersion in underground roadway

Lihai Tan
University of Wollongong, lt716@uowmail.edu.au

Ting X. Ren
University of Wollongong, tren@uow.edu.au

Coupled cfd-dem modelling of mine dust dispersion in underground roadway

Abstract

Dust particles floating inside roadways are characterized by various sizes. However, it is difficult to replicate the dust environment with such factors taken into consideration in laboratory experiments. Fortunately, computational technology provides an alternative way for that. In this study, in order to investigate the movement mechanism of dust with different diameters from heading face in the underground roadway, a three-dimensional CFD-DEM coupling numerical model is presented using the Eulerian-Lagrangian method. A numerical roadway model based on a practical engineering case has been established for the purpose of studying the dust diffusion under single-forced ventilation condition in roadway underground. The study suggests that particle size has a significant effect on dust dispersion. The results demonstrate that CFD-DEM coupling computational simulation can be an effective approach for the investigation of dust issues in underground engineering.

Disciplines

Engineering | Science and Technology Studies

Publication Details

Tan, L. & Ren, T. (2019). Coupled cfd-dem modelling of mine dust dispersion in underground roadway. Mining Goes Digital - Proceedings of the 39th international symposium on Application of Computers and Operations Research in the Mineral Industry, APCOM 2019 (pp. 612-619). London: Taylor & Francis Group.

Coupled CFD-DEM modelling of mine dust dispersion in underground roadway

Lihai Tan
School of Civil, Mining and Environmental Engineering, University of Wollongong, NSW 2522, Australia

Ting Ren
School of Civil, Mining and Environmental Engineering, University of Wollongong, NSW 2522, Australia

ABSTRACT: Dust particles floating inside roadways are characterized by various sizes. However, it is difficult to replicate the dust environment with such factors taken into consideration in laboratory experiments. Fortunately, computational technology provides an alternative way for that. In this study, in order to investigate the movement mechanism of dust with different diameters from heading face in the underground roadway, a three-dimensional CFD-DEM coupling numerical model is presented using the Eulerian-Lagrangian method. A numerical roadway model based on a practical engineering case has been established for the purpose of studying the dust diffusion under single-forced ventilation condition in roadway underground. The study suggests that particle size has a significant effect on dust dispersion. The results demonstrate that CFD-DEM coupling computational simulation can be an effective approach for the investigation of dust issues in underground engineering.

1 INTRODUCTION

Dust pollution is one of the most serious issues in coal mining underground. With the popularity of mechanical mining, dust is becoming a major hazard threating worker's health and equipment safety(Petsonk et al., 2013). Various dedusting methods have been developed in order to solve the dust concentration problem, among which ventilation is regarded as one of the most practical ways for dust reduction. Undoubtedly, understanding the migration and distribution of dust particles is of great importance for dust control by ventilation. It has long been known that both the hazard level of dust on human health and explosion risk largely depend on the size of dust(Sapko et al., 2007). Dust with smaller sizes is more likely to enhance the explosion risk, especially for those whose particle diameter is less than 200um.

Various dedusting methods have been developed in order to solve the dust concentration problem, among which ventilation is regarded as one of the most practical ways for dust reduction. Undoubtedly, understanding the migration and distribution of dust particles is of great importance for dust control by ventilation. As an alternative methodology, Computational Fluid Dynamics (CFD) numerical simulation has been extensively employed; as it can investigate the dust dispersion and airflow overall, and is easy to replicate practical cases and ventilation conditions with much less geometry and size constraints. Over the past years, extensive studies have been performed on dust dispersion in coal mines using the CFD method. Toraño investigated the evolution of airflow and dust flow field in a roadway with forced-exhaust ventilation system using the CFD method whose feasibility and accuracy have been perfectly proved by in-site measurements(Toraño et al., 2011). Wang numerically investigated the dust movement and dust distribution with hybrid ventilation system and the results show an uneven distribution of dust in the laneway(Wang et al., 2015). Kurnia employed the CFD method to evaluate various methods used for mitigating dust dispersion from the mining face and determined the most effective one(Kurnia et al., 2014). Wang simulated the dust in a roadway with a curtain of air curtain installed on the shearer using the CFD method and the results show that the air curtain can effectively reduce the dust concentration on the side of the operator(Pengfei et al., 2011). Parra examined three different

types of ventilation systems (blowing, exhaust and mixed ventilation) using the CFD method and this numerical study was validated by the measurements taken in a real mine gallery(Parra et al., 2006).

All of the above studies using the CFD method show that the distribution and movement of dust are affected obviously by the airflow field. However, most of them mainly pay their attention to the dust dispersion at a macro-scale; as the CFD method is difficult to reveal the movement characteristics of particles from a microscopic viewpoint. Recently, CFD-DEM (computational fluid dynamics and discrete element method) coupling method has been under development for numerical simulation with fluid-solid two-phase flows involved. Using this method, the airflow is simulated and investigated by the traditional CFD method while the simulation of particles is performed by the DEM method; thus allowing the interaction between fluid and solid to be considered. Therefore, the motion of any particle in the airflow can be tracked and its migration can be accurately determined. Moreover, this method requires less empirical parameters and affords the ability to clearly present the particle trajectory and the interaction between particle and fluid(Yu et al., 2018).

In this study, an airflow-dust model was established using a CFD-DEM coupling method. The dispersion process of dust particles in a roadway installed with single-forced ventilation system was numerically simulated and the effect of particle size on dust dispersion and distribution was analysed. The aim of this study is to improve the understanding of dust dispersion mechanism and present the performance of the CFD-DEM coupling method on studying the particle migration in airflow.

2 NUMERICAL MODELLING OF AIR-DUST COUPLED FLOW

In this study, Eulerian-Lagrangian method was employed to track the particle trajectory in the airflow. As the total volume of particles was far smaller than that of the fluid, which caused little force of dusts on airflow, one-way coupling modelling was employed, which means that the influence of dusts on airflow was not taken into consideration. As the sphere is the most typical shape of dust, spherical dust particles with different sizes were considered. Spherical particles with diameters of 20 um, 40 um, 60 um and 80 um were created to analyse the size effect.

The prototype of the numerical roadway model was a typical three-centred arch roadway underground in a coal mine. The dimension of the roadway was 3.7 m ×3.4 m×40.0m (width × height × length). Single-forced ventilation system was used for dust removal in the roadway. The ventilation duct with a diameter of 0.6 m, whose centre axis was 2.6 m away from the floor and 1.2 m away from the tunnel centre axis along Z axis, was 10.0 m away from the heading face. Forced air capacity was 260 m^3/min, affording a ventilation velocity of 15.33m/s. The initial dusts were assumed to be distributed statically and uniformly inside the dust zone within 1.0 m of the heading face.

The time-step, which has a positive correlation with particle's size and density and a negative correlation with particle's stiffness, must be small enough for an accurate result. In this study, the DEM time-step was set as 1.2×10^{-7} s in accordance with the smallest particle. k-ε model was used to describe the air turbulent flow in the airflow field. The interaction of particle to particle was described by the Hertz-Mindlin (no slip) model and the interaction between particles and wall by the Hertz-Mindlin with JKR model. Other key parameters are listed in Table 1. Before CFD-DEM coupling with dust created, the ventilation was performed for 120 seconds and the airflow field was stable.

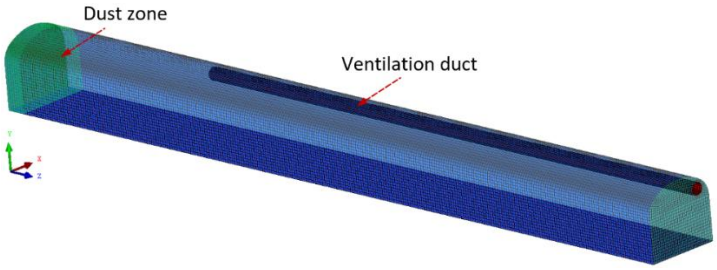

Figure 1. The numerical model of the roadway

Table 1 Parameters for the CFD-DEM coupling simulation

Properties		Values	Properties	Values
Dust	Density	1400 kg/m^3	Ventilation velocity	15.33 m/s
	Poisson's ratio	0.5	Turbulent intensity	5.0%
	Shear modulus	1×10^8 Pa	Time step (CFD)	1.0×10^{-4} s
Air	Density	1.225 kg/m^3	Time step (DEM)	1.2×10^{-7} s
	Viscosity	1.789×10^{-5} m^2/s	Gravity	9.8m/s^2

3 ANALYSIS OF RESULTS

3.1 *Airflow field*

The velocity streamlines for the airflow at the dispersion time of 0.0s are presented in Figure 2. According to Yu's research, the airflow field was suggested to be classified into three regions: vortex region, multi-direction turbulence region and stable region(Yu et al., 2018). This classification method is also applied in this study. As shown in Figure 2, air was jetted out from the ventilation duct rapidly, forming a high-velocity strip airflow field extending to the heading face, and then the airflow flowed against the heading face to the other side and turned back towards the roadway exit. The region between the heading face and ventilation duct was regarded as the vortex region. In this region, the airflow slowed down quickly with ventilation velocity decreasing from 15.33 m/s to about 3.5 m/s due to energy loss. Afterwards, air flowed into the multi-direction turbulence region with a length of about 16.0 m, where the airflow was somewhat disordered and decelerated continuously. Eventually, the airflow decelerated to the lowest level of less than 0.5m/s, becoming stable and parallel to the axes of the roadway in the stable region.

As shown in Figure 3, in the vortex region, the ejected air resulted in the high-speed airflow concentration in front of the outlet of the ventilation duct, then the rebounded airflow formed another high-speed airflow concentration in the lower area close to the floor (Z=5.0m). In the turbulence region, high-speed airflow firstly concentrated at the side opposite to the ventilation duct and then migrated to the upper area of the roadway (Z=15.0m and Z=20.0 m). In the stable region, the velocity of airflow had been slowed down to the lowest level (Z=30.0m and Z=35.0 m).

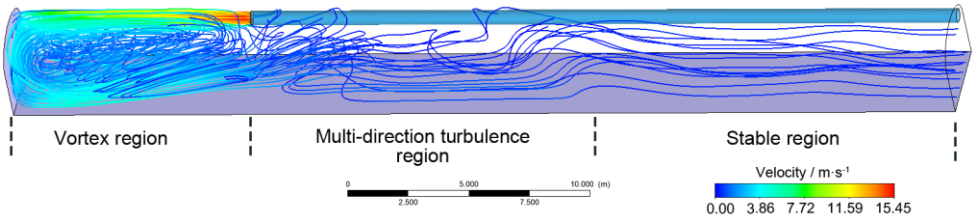

Figure 2. Velocity field of airflow in the roadway

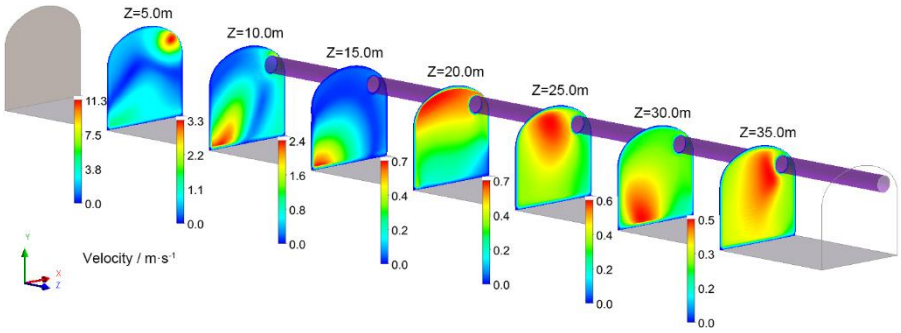

Figure 3. Velocity field sections of airflow in the roadway

3.2 *Migration of particles with different sizes*

In the numerical model, the positive direction of the Z axis denotes the direction from the heading face to the roadway exit along the long axis of the roadway. Therefore, the dispersion velocity for different kinds of dust particles was defined as their average Z velocity. The dispersion velocity of spherical dust particles with different sizes is presented in Figure 4. It can be seen that the dispersion velocity of all particles soared dramatically at first and reached a climax of about 3.7 m/s when dispersion time was roughly 2.1 s. Subsequently, the average dispersion velocity dropped sharply to the lowest level for all dust particles. It should be noticed that average dispersion velocity for participles with diameter of 20um and 40um turned to be negative for a while with lowest velocity of -0.67m/s and -0.33m/s, respectively. At post-peak stage, obvious velocity fluctuation can be observed for particles with diameters of 20 um and 40 um. However, the post-peak dispersion velocity of dust particles with greater diameters (60 um and 80um) was much stable and levelled off at about 0.4 m/s.

The difference of dispersion velocity caused different dust dispersion distances, which is shown in Figure 5. Turning points for dusts with different sizes appeared simultaneously when dispersion time was 5.0s, which lagged behind the time when dispersion velocity reached its peak. Each dispersion evolution curve can be divided into two parts. Before the turning point, dispersion curves rose quickly and almost coincident with each other. When dispersion time reached the turning point, the curves began to get flatter and went up linearly. The average distance gap between dust particles also widened gradually. In general, dust particles with greater sizes migrated further along the long axis of the roadway than those with smaller sizes. When dispersion time was 30.0s, the average dispersion distance for dust particles with diameter of 80um was 22.2m while for those with diameter of 20um was only 15.7m.

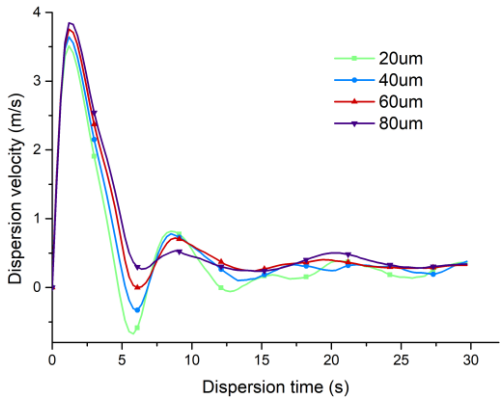

Figure 4. The dispersion velocities of spherical dust particles with different sizes

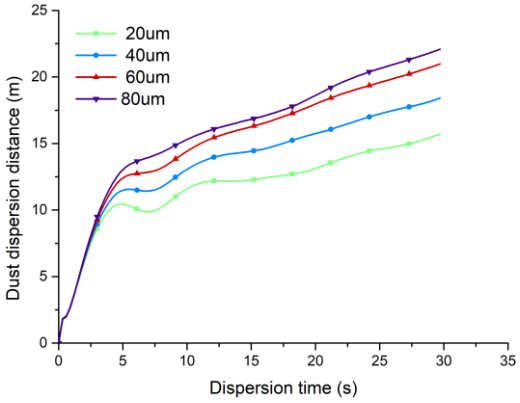

Figure 5. The average dispersion distance of spherical dust particles with different sizes

Figure 6 presents the distribution of dust particles with different sizes at different dispersion times. The particles with different diameters are represented by different colours. As the size of dust particles was far smaller compared with that of the roadway, all the dust particles had been amplified for better observation. For the purpose of better understanding the dust distribution characteristics, the projection of dust distribution in the XY plane and ZY plane are presented in Figure 7 and Figure 8 respectively.

At the beginning of dispersion (DT=1.0s), all particles near the heading face were dragged down and moved forward with the rebounded airflow. When DT=5.0s, some dust particles, the majority of whom were small particles with diameters of 20um and 40um, were sucked into the airflow ejected from the ventilation duct and then dragged back to the vortex region because of the strong negative pressure around the outlet of the ventilation duct. Afterwards, more and more dust particles were dragged back when approaching to the outlet of the ventilation. When DT=8.0s, a dust backflow loop had been formed. The backward dust particles flew with the ejected airflow and repeated the trajectory from the heading face. There was a possibility for them to get rid of the vortex region at the end of the circulation. With the increase of dispersion time, an increasing number of dust particles had escaped from the vortex region and entered the stable region. When DT=30.0s, most dust particles had been got out of vortex region while only few of them, which were mainly small particles with diameters of 20um and 40um, were still flowing in the circulation.

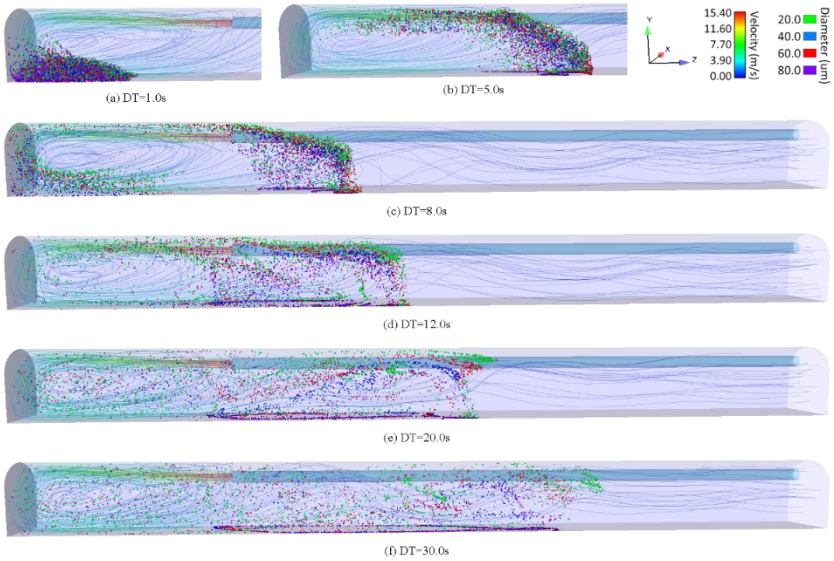

Figure 6. The migration of dust particles with different sizes at typical dispersion times

The plane projections clearly illustrate the distribution difference between dust particles with different sizes. Smaller dust particles were more likely to flow above larger dust particles. During dispersion time from 8.0s to 30.0s, we can see that dust particles could be roughly divided into four height levels with the smallest particles with diameter of 20um migrating at the highest level and the largest particles with diameter of 80um at the lowest one. It is also obvious that the influence of gravity over particles was sensitive to particle size. As shown in Figure 8, when DT=1.0s, a considerable portion of dust particles with diameter of 80um settled on the floor, then rose again with strong airflow. Overall, settled dust particles, most of whose diameter was 80um, were mainly distributed in the area more than 9.0m away from the heading face. There was no obvious settlement of dust particles with diameters of 20um and 40um.

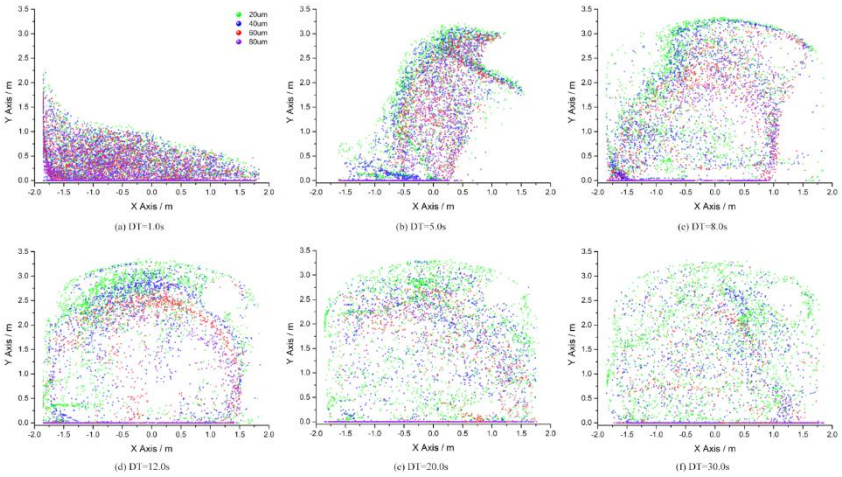

Figure 7. The projection of dust distribution on XY plane at typical dispersion times

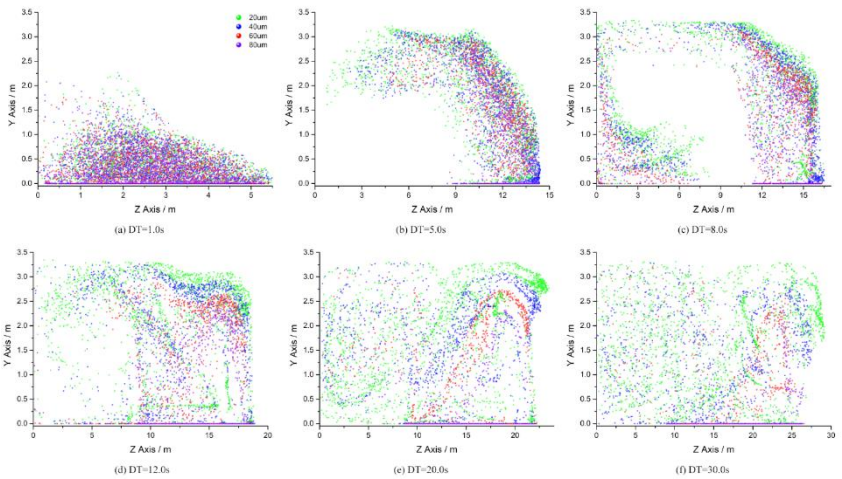

Figure 8. The projection of dust distribution on ZY plane at typical dispersion times

4 DISCUSSIONS AND CONCLUSIONS

According to the evolution of dust dispersion velocity, four stages in the process of dispersion can be classified under the single-forced ventilation condition as shown in Figure 9. The scattered points denote the velocities of different kinds of dust particles and the black dash line denotes their average value.

(1) Accelerative dispersion stage

High-speed airflow ejected from the ventilation duct and rebounded when reaching the heading face, forming a vortex airflow field between ventilation duct and heading face. Therefore, at the beginning of dispersion, the dust particles near the heading face accelerated rapidly because of the strong drag force from the rebounded airflow.

(2) Deceleration dispersion stage

The velocity of the rebounded airflow suffered a sharp decrease in a short distance. Accordingly, the dust particles slowed down rapidly. Moreover, in this period, a number of particles were sucked into the circulation in the vortex region. Consequently, the overall dispersion velocity experienced a drastic drop.

(3) Fluctuant stage

In this stage, a large proportion of the dust particles had migrated into the turbulence region and the rest of them was still bound in the vortex region. Overall, the dispersion velocity was fluctuant at a lower level.

(4) Stable dispersion stage

As the airflow flew into the stable region, most of the dust particles began to migrate in a stable dispersion velocity until flowing out from the roadway.

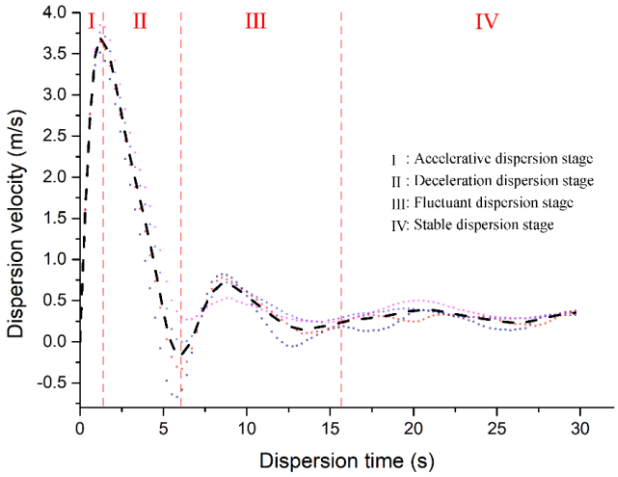

Figure 9. The average dispersion velocities of all dust particles

For the dust particles investigated in this study, particles with greater diameters were easier to disperse forward than those with smaller diameters. This may be attributed to their better motion stability in the airflow. The smaller dust particles are more susceptible to the airflow characterized by instability before entering the stable region. As a result, their motion is less orderly. It has been observed in this study that the smaller dust particles are more likely to be affected by the entrainment effect of the high-speed ejected airflow and therefore there is a high possibility of getting incorporated into the dust circulation for them.

Dust particles mainly settled in the multi-direction turbulence region and stable region where the airflow speed was much less than that in the vortex region. In this study, for larger dust particles with diameters of 60um and 80um, they were more likely to migrate at a lower height and settle compared with those of diameters of 20um and 40um due to the effect of gravity, which means that smaller dust particles are more responsible for dust pollution.

REFERENCES

KURNIA, J. C., SASMITO, A. P. & MUJUMDAR, A. S. (2014) Dust dispersion and management in underground mining faces. *International Journal of Mining Science and Technology,* 24**,** 39-44.

PARRA, M., VILLAFRUELA, J., CASTRO, F. & MENDEZ, C. (2006) Numerical and experimental analysis of different ventilation systems in deep mines. *Building and Environment,* 41**,** 87-93.

PENGFEI, W., TAO, F. & RONGHUA, L. (2011) Numerical simulation of dust distribution at a fully mechanized face under the isolation effect of an air curtain. *Mining Science and Technology (China),* 21**,** 65-69.

PETSONK, E. L., ROSE, C. & COHEN, R. (2013) Coal mine dust lung disease. New lessons from an old exposure. *American journal of respiratory and critical care medicine,* 187**,** 1178-1185.

SAPKO, M. J., CASHDOLLAR, K. L. & GREEN, G. M. (2007) Coal dust particle size survey of US mines. *Journal of Loss Prevention in the Process Industries,* 20**,** 616-620.

TORAÑO, J., TORNO, S., MENÉNDEZ, M. & GENT, M. (2011) Auxiliary ventilation in mining roadways driven with roadheaders: validated CFD modelling of dust behaviour. *Tunnelling and Underground Space Technology,* 26**,** 201-210.

WANG, Y., LUO, G., GENG, F., LI, Y. & LI, Y. (2015) Numerical study on dust movement and dust distribution for hybrid ventilation system in a laneway of coal mine. *Journal of Loss Prevention in the Process Industries,* 36**,** 146-157.

YU, H., CHENG, W., XIE, Y. & PENG, H. (2018) Micro-scale pollution mechanism of dust diffusion in a blasting driving face based on CFD-DEM coupled model. *Environmental Science and Pollution Research***,** 1-21.